ACS APPLIED MATERIALS & INTERFACES

Research Article

www.acsami.org

Optically Controllable Dual-Gate Organic Transistor Produced via Phase Separation between Polymer Semiconductor and Photochromic Spiropyran Molecules

Yasushi Ishiguro,[†,‡] Ryoma Hayakawa,[‡] Toyohiro Chikyow,[‡] and Yutaka Wakayama*[,†,‡]

[†]Department of Chemistry and Biochemistry, Faculty of Engineering, Kyushu University, 1-1 Namiki, Tsukuba 305-0044, Japan

[‡]International Center for Materials Nanoarchitectonics (WPI-MANA), National Institute for Materials Science (NIMS), 1-1 Namiki, Tsukuba 305-0044, Japan

Supporting Information

ABSTRACT: We produced an optically controllable dual-gate organic field-effect transistor by a simple one-step spin-coating of a mixed solution of photochromic spiropyran (SP) and poly(3-hexylthiophene) (P3HT). Postannealing enhanced polymer chain ordering of P3HT to induce phase separation into an SP-rich lower layer and an SP-free upper layer. These layers worked independently as transistor channels with distinct optical responsivity. The top channel was optically inactive, but the bottom channel was optically active, because of the photoisomerization of SP. These results demonstrate the potential of our technique to produce a multifunctional photoactive organic transistor by a simple process.

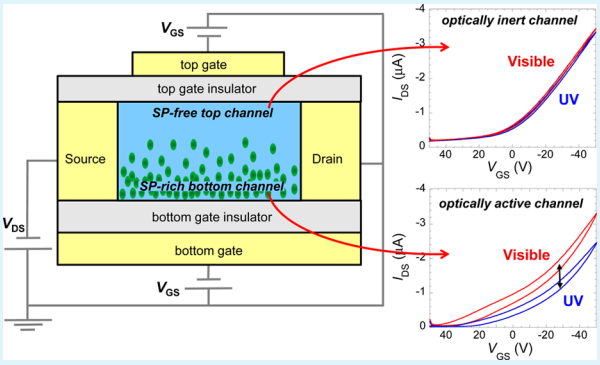

KEYWORDS: *organic field-effect transistor, photochromism, phase separation, optically controllable transistor, spiropyran, poly(3-hexylthiophene)*

1. INTRODUCTION

Chemical doping is an effective technique for improving the performance of organic devices.[1−4] Electron donor or acceptor molecules, such as tetrafluorotetracyanoquinodimethane, $FeCl_3$, and MoO_3, have been doped into host semiconductors to increase the density of charge carriers. Chemical doping can increase carrier mobilities of organic field-effect transistors (OFETs).[5−10] Doping MoO_3 into a pentacene channel layer improved the carrier mobility from 0.71 to 1.60 $cm^2\ V^{-1}\ s^{-1}$.[5] Chemical doping also offers a useful way to integrate new functionalities into conventional OFETs. For instance, optically controllable OFETs have been developed by doping photoisomerization molecules such as spiropyran (SP) and diarylethene.[11−18] In these studies, the transistor properties were optically modulated by photoisomerization.

Generally, the dopant concentration should be as high as possible to maximize the doping effect. However, there is an upper limit to the dopant concentration to avoid phase separation or dopant segregation, which can degrade transistor properties and hinder the dopant effect. For example, Li et al. had to restrict the SP concentration in host poly(3-hexylthiophene) (P3HT) to <10 wt % to suppress phase separation.[11] To solve this issue, we used poly(triarylamine) (PTAA) as a host polymer in our previous study,[19] because PTAA has an amorphous structure and allows doping with up to 50 wt % SP. Furthermore, we achieved multilevel switching of the drain currents with an optical memory effect by stacking an optically active SP−PTAA layer and an optically inactive neat PTAA layer to form a dual-gate OFET.[20] However, the high solubility of SP molecules in PTAA necessitated a complicated process, including several spin-coating steps and the deposition of an aluminum oxide film.

Here, we intentionally promoted phase separation and made the most of the dopant segregation to produce a multifunctional dual-gate transistor. To facilitate phase separation, we used crystalline P3HT as a host polymer.[21] Phase separation of the SP−P3HT blend film induced segregation of SP molecules around the base of the film, and we fabricated a dual-gate OFET from this phase-separated blend film. This simple one-step process simultaneously created distinct optical responsivities between the top and bottom channels. The bottom channel was optically active because of the photoisomerization of SP, but the top channel was inactive, because of the absence of the SP molecules in the upper part of the blend film. Our approach makes it possible to fabricate multifunctional dual-gate OFETs simply.

2. EXPERIMENTAL SECTION

Figure 1 illustrates the configuration of a dual-gate transistor and the chemical structures of P3HT and SP molecules. The SP molecules

Received: March 31, 2014
Accepted: June 9, 2014
Published: June 9, 2014

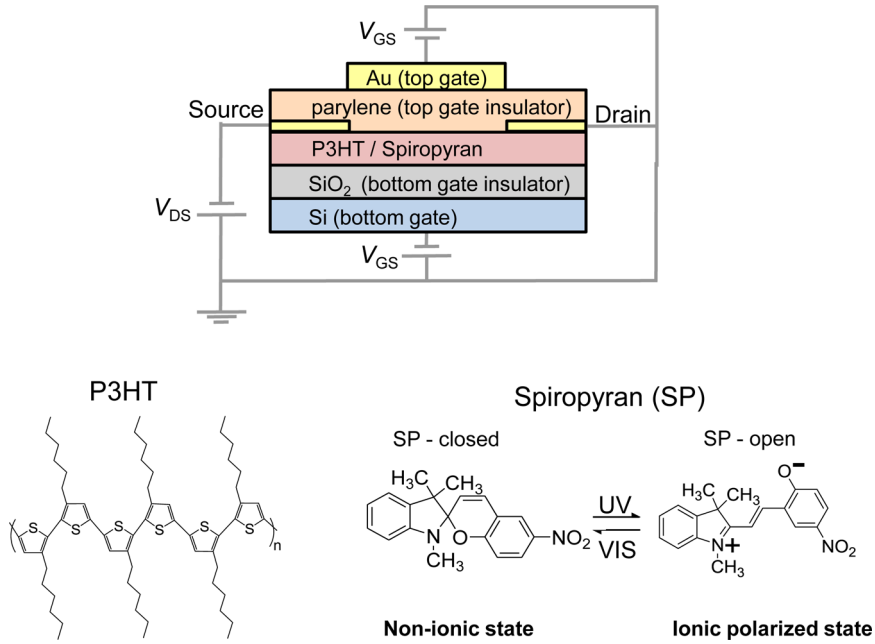

Figure 1. Schematic illustrations of the dual-gate transistor and the chemical structures of P3HT and spiropyran. The open-ring isomer of spiropyran reversibly transforms into the closed-ring isomer and vice versa by alternating UV−vis irradiation. The open ring has an ionic polarized state, while the closed ring has a neutral structure.

undergo a reversible conformational change upon UV−vis light irradiation. The closed-ring isomer is nonionic, whereas the open-ring isomer has an ionic polarized state. Highly doped p-type Si wafers with a 200 nm thick SiO_2 layer were used as substrates. The Si substrate and SiO_2 layer work as a gate electrode and an insulator layer of the bottom channel transistor, respectively. A 1:1 (weight ratio) mixture of P3HT and SP dissolved in chlorobenzene at 1 wt % was spin-coated (1000 rpm for 1 min at room temperature) on the substrate. The samples were then annealed at 70 °C for 12 h in a nitrogen atmosphere to enhance the chain ordering of P3HT. The layer thus prepared works as the transistor channels. The thickness of the thermally annealed SP−P3HT film was estimated to be 53 nm with a surface profilometer (Dektak 6M). On top of the SP−P3HT film, interdigitated Au electrodes were deposited as source and drain electrodes through a metal shadow mask. The transistors had a channel length of 100 μm and a width of 51 mm. Subsequently, parylene-C was deposited by chemical vapor deposition as a top gate insulator. The thickness of the film was estimated to be 1.3 μm. Finally, a 20 nm thick Au electrode was deposited on the parylene-C film as the top-gate electrode through a metal shadow mask.

The electrical characteristics of the transistors were measured at room temperature with a semiconductor device analyzer (Agilent B1500A). For dual-gate operation, the bottom gate is grounded while the top channel is operated, and vice versa. A xenon lamp was used as the light source for the photoisomerization of the SP. Band-pass filters passed UV light at 340 nm (0.10 mW/cm^2 by power meter) to generate the ionic polarized open-ring isomer and visible light at 550 nm (1.10 mW/cm^2) to transform the open-ring isomer into the nonionic closed-ring isomer. The light irradiation time was fixed at 10 min. This duration and the light intensity were selected to inhibit photocurrent or photo-oxidation, but to still induce SP photo-isomerization in the P3HT matrix. The characteristic variation in the absorption band around 550 nm observed under these conditions confirms the reversible photoisomerization of SP in the P3HT matrix (Figure S2, Supporting Information). The absorption peak clearly agreed with that of the open-ring isomer of SP (Figure S1a, Supporting Information). In contrast, no change in the absorption peak from that of P3HT was observed (Figure S1b, Supporting Information). These results clarified that the photoisomerization of SP takes place in the P3HT film.

Electrical measurements and light irradiation were conducted in a vacuum chamber (10^{-1} Pa) to eliminate the influence of atmosphere, particularly of ozone gas generated by UV light.

The depth profile of the SP molecules in P3HT was examined by time-of-flight secondary ion mass spectrometry (TOF-SIMS). An argon gas cluster ion beam (Ar-GCIB) was used to etch the samples, and Bi^{3+} ions were used for ionizing sputtered species. The SP−P3HT film was prepared on the SiO_2/Si substrate under the same conditions that were used for the transistors. The crystallinity of the P3HT films was investigated with an X-ray diffractometer (XRD, Bruker D8 Discover; Cu Kα source, λ = 0.15418 nm).

3. RESULTS AND DISCUSSION

First, we evaluated the basic transistor properties of the dual-gate transistor. Figure 2 shows the output characteristics obtained from the top and bottom channels. Both sets of output curves clearly display p-type characteristics, indicating that both the upper and lower sides of the P3HT−SP blend film worked as transistor channels.

The carrier mobility and threshold voltage were estimated from the saturation regime in the transfer curves (see Figure

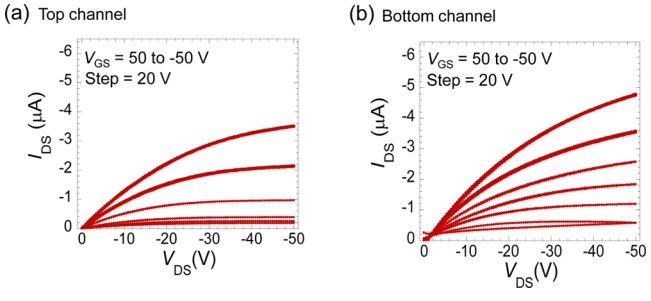

Figure 2. (a) Output characteristic in the top channel (while the bottom gate is grounded). (b) Output characteristic in the bottom channel (while the top gate is grounded). The carrier mobility of the bottom channel was 1 order of magnitude lower than that of the top channel.

S3a,b, Supporting Information). Here, the capacitances of top and bottom gate insulators were 18.5 nF/cm^2 for SiO_2 and 2.34 nF/cm^2 for parylene-C. Clear differences were observed in the carrier mobilities and threshold voltage. The carrier mobility of the bottom channel (7.5×10^{-5} cm^2 V^{-1} s^{-1}) was 1 order of magnitude lower than that of the top channel (9.6×10^{-4} cm^2 V^{-1} s^{-1}). In addition, the threshold voltage of the bottom channel (59 V) was higher than that of the top channel (31 V).

Second, we examined the effect of light irradiation on the transistor properties. Figure 3a shows the transfer characteristics of the top channel at a constant drain bias voltage (V_{DS} = −50 V) with alternating UV−vis irradiation. There was no change in the drain current; i.e., the top channel is inactive under light exposure. In contrast, the drain current through the bottom channel was reduced by UV irradiation and restored by visible irradiation, indicating that the bottom channel is optically active (Figure 3b). It is noteworthy that hysteresis was observed only in the bottom channel.

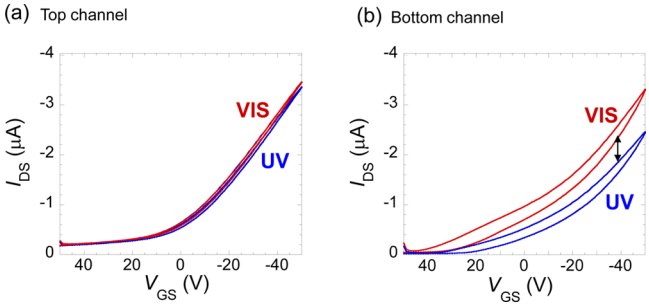

Figure 3. (a) Transfer characteristics of the top channel at a V_{DS} of −50 V under UV or visible irradiation for 10 min. No change was observed under light exposure. (b) Reversible change in transfer characteristics of the bottom channel at a V_{DS} of −50 V by alternating UV−vis irradiation. Hysteresis was observed only in the bottom channel.

Finally, we investigated the variations in the maximal drain current ($I_{DS,max}$), carrier mobilities, and threshold voltages upon UV−vis irradiation to improve our understanding of the effect of irradiation on the transistor properties. Figure 4a plots changes in $I_{DS,max}$ at a gate-source bias voltage (V_{GS}) of −50 V at each channel with repeated UV−vis irradiation. The optical responsivity differs clearly between channels. In the top channel, the drain current showed an only marginal change upon irradiation. In the bottom channel, in contrast, UV irradiation reduced $I_{DS,max}$ by ∼30%, and several cycles of optical switching were observed, during which time the drain current gradually decreased. This degradation in the switching property can be ascribed to the deterioration of SP molecules upon irradiation.[22,23] Panels b and c of Figure 4 show changes in carrier mobilities (μ) and threshold voltages (V_{th}) estimated from the saturation regime in the transfer curves of each channel under repeated UV−vis irradiation. Typical $|I_{DS}|^{1/2}$ versus V_{GS} plots used for the calculation of μ and V_{th} are shown in Figure S2 (Supporting Information). In the bottom channel, UV irradiation decreased the carrier mobility by 10%, from 7.5×10^{-5} to 6.8×10^{-5} cm^2 V^{-1} s^{-1}, and reduced the threshold voltage from 59 to 45 V. In the top channel, in contrast, these values were almost constant regardless of UV or visible irradiation.

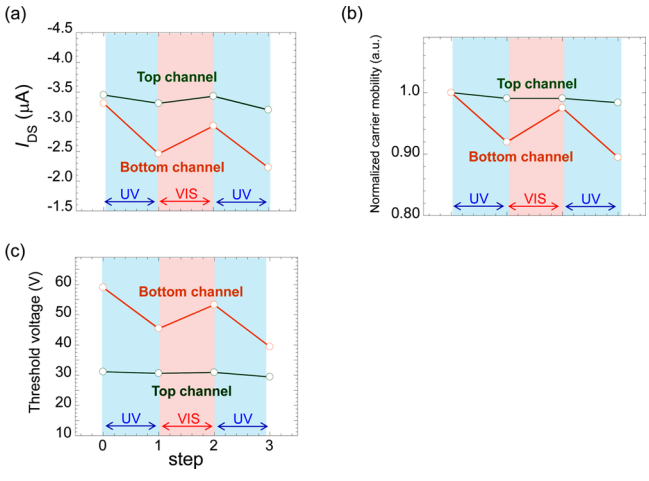

Figure 4. Variations in transistor properties in top and bottom channels dependent on light irradiation: (a) drain current at V_{DS} = −50 V and V_{GS} = −50 V, (b) carrier mobility (μ) normalized to the initial value, and (c) threshold voltage (V_{th}).

These results imply that the SP molecules were distributed mainly around the bottom channel. To provide clear evidence of the distribution of SP molecules in the P3HT layer, we performed TOF-SIMS measurement by Ar-GCIB.[24] The depth profiles of the SP, P3HT, and SiO_2 molecules are shown in Figure 5a. The fragment ions of $C_{18}H_{15}N_2O_3^-$, C_2HS^-, and SiO_2^- originated from SP, P3HT, and SiO_2 substrate, respectively. The intensity of $C_{18}H_{15}N_2O_3^-$ increased from the surface by 2 orders of magnitude and reached the maximum at a depth of 25 nm. On the other hand, the intensity of SiO_2^- started increasing from a depth of 25 nm and saturated at a depth of ∼65 nm. That is, the magnitude of the signal from the substrate started increasing at the depth at which the magnitude of the signal from the SP molecules reached its maximum. From these results, we conclude that SP molecules are segregated mostly near the interface between the P3HT and the SiO_2 substrate. The differences in carrier mobilities, threshold voltages (Figure 2), and electrical hysteresis in the bottom channel (Figure 3b) can be ascribed to the highly concentrated SP molecules around the bottom channel. The gradual onset of the intensity of SiO_2^- over a depth range of 30−50 nm is probably caused by the surface roughness of the SP−P3HT film; in fact, atomic force microscopy showed many dimples ∼20 nm deep across the surface (Figure 5b).

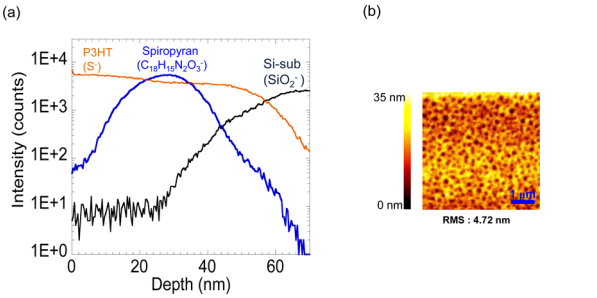

Figure 5. (a) Depth profiles of negative ions ($C_{18}H_{15}N_2O_3^-$ from spiropyran, S^- from P3HT, and SiO_2^- from the substrate) collected by using a 30 keV Bi^{3+} source. Samples were eroded with an Ar gas cluster ion beam at 5 keV. (b) Atomic force microscope image of the SP−P3HT blend film.

dx.doi.org/10.1021/am501884q | ACS Appl. Mater. Interfaces 2014, 6, 10415−10420

The segregation of SP molecules in the P3HT matrix is presumably facilitated by chain ordering of P3HT through thermal annealing in the same manner seen for the blends of crystalline semiconductor with an amorphous insulator or an amorphous semiconductor.[25−31] Figure 6 shows XRD spectra

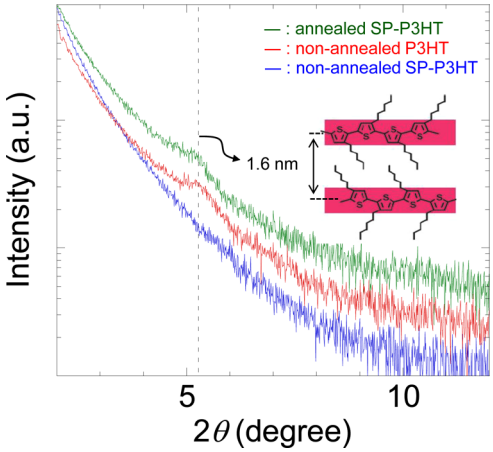

Figure 6. X-ray diffraction spectra obtained from the annealed SP−P3HT blend film, the nonannealed pristine P3HT film, and the nonannealed SP−P3HT blend film. A diffraction peak indicated by the dashed line corresponds to the interchain lattice constant.

measured from nonannealed pristine P3HT and SP−P3HT blend films and an annealed SP−P3HT blend film. The (100) diffraction peak at $2\theta \approx 5.2°$ from the nonannealed P3HT film is indicated by a dashed line, but no peak was observed from the nonannealed SP−P3HT blend film. That is, the P3HT film basically has ordered structure, but doping of SP molecules disturbs the alignment of the P3HT chains. On the other hand, the postannealing on the SP−P3HT blend film yielded the peak at $2\theta \approx 5.2°$. This result shows that thermal annealing induced the ordering of P3HT. Therefore, we consider that the chain ordering of P3HT through thermal annealing involves the segregation of SP molecules around the bottom layer.

As a reference, we evaluated optical responsivity in a dual-gate transistor made from a nonannealed SP−P3HT film. Both top and bottom channels were optically active and showed only a slight difference: the UV-induced reductions in $I_{DS,max}$ were 0.5 μA in the top channel and 0.7 μA in the bottom channel (Figure S4, Supporting Information). These results clarify that the distribution of SP molecules was originally uniform in the nonannealed blend film, and annealing was responsible for the clear difference in optical responsivity between channels. These results support the view that thermal annealing promotes the alignment of P3HT chains as well as the segregation of SP molecules.

We measured the depth profile of SP in the PTAA film to confirm our results. Unlike P3HT, PTAA forms an amorphous structure. The concentration of SP was 50 wt %, and we used the same annealing process that was used for the SP−P3HT film. The intensity of $C_{18}H_{15}N_2O_3^-$, which is derived from SP molecules, was constant through the film (Figure S5, Supporting Information). The onset of SiO_2^- was relatively steep, and no surface morphology was visible in the atomic force microscope image. These results show that SP molecules are homogeneously distributed in the amorphous PTAA matrix to form the SP−PTAA film with a uniform thickness. They also support the view that the ordering of P3HT chains is essential for SP molecules to segregate near the bottom channel. Although the reason why SP molecules are segregated near the bottom of P3HT film is still unclear, a possible reason is that the segregation would be induced by the difference in the wettability of P3HT and SP. We examined the wettability of respective films. The respective contact angles were 98° for P3HT and 55° for SP (Figure S6, Supporting Information); the wettability of SP is higher than that of P3HT. Accordingly, SP molecules would be segregated near the hydrophilic SiO_2 surface.

In previous work, we produced an optically controllable dual-gate OFET by stacking an optically active SP-doped PTAA layer and a nondoped inactive PTAA layer, demonstrating multilevel switching with an optical memory effect.[20] As the SP−P3HT-based dual-gate transistor developed here has the same device configuration, the same device operation (i.e., multilevel switching with a memory effect) can be expected, but via a much simpler one-step spin-coating process. In general, concentrations of chemical dopants are confined within limits to avoid phase separation or dopant segregation.[11,12] In contrast, we intentionally promoted phase separation and made the most of dopant segregation. This approach fosters the simple fabrication of multilayered, multifunctional dual-gate OFETs.

Finally, we discuss the optical switching mechanism. In our previous study, we observed the same optical switching behaviors in the SP−PTAA system: drain currents and carrier mobilities decreased with UV irradiation and recovered with visible irradiation.[19] We elucidated that the ionic polarized state of the open-ring SP molecules worked as carrier scattering sites to reduce drain current. The SP−P3HT system showed similar optical responsivity here. Therefore, the same switching mechanism (i.e., carrier scattering by ionic SP molecules) works in the SP−P3HT system.

Li et al. reported similar optical switching via the use of an SP−P3HT blend film as a transistor channel,[11] although UV irradiation increased the drain current and visible irradiation restored it. The important point is that the photocurrent was optically switched in their study. The photoexcited electrons in P3HT were collected in the drain electrode via the lowest unoccupied molecular orbital (LUMO) of SP. The reversible change in the LUMO level of the SP molecules was the origin of the switchable electron transfer. Thus, the photocurrent switching overlapped the base drain current. This explains the narrow range of the on:off ratio. For these reasons, their switching behavior and mechanism were fundamentally different from ours. Orgiu et al. created an optically controllable transistor by doping photochromic diarylethene molecules into P3HT to work as hole trap sites.[12] The reversible variation in the highest occupied molecular orbital (HOMO) level of the diarylethene triggered optical switching of the drain currents. As both studies show, the combination of dopants and polymer must be carefully selected, because the relative positions of the energy level between photochromic dopants and the host polymer are essential for optical control.

In contrast, our carrier scattering mechanism can be widely applied to any polymer matrix, unlike the carrier trapping (or transfer) mechanism through HOMO−LUMO levels of host polymer and photochromic dopants,[11,12] because the electric charge of ionic polarized SP molecules can affect the carrier transport regardless of the relative energy level positions. In fact, we observed consistent optical switching behaviors in both SP−PTAA[19] and SP−P3HT blends. Therefore, we conclude

that the scattering mechanism also holds in this study. To be exact, V_{th} values were changed by irradiation of this SP−P3HT film, although the SP−PTAA film showed no change upon UV−vis irradiation. However, V_{th} values changed also in SP−PTAA blends if the SP concentration exceeded 70 wt % (Figure S7, Supporting Information). These results confirm the consistency of the scattering mechanism in both blend combinations.

4. CONCLUSIONS

We present a new approach for the fabrication of optically controllable dual-gate OFETs based on phase separation. The dopant SP molecules were distributed mainly near the bottom channel through phase separation, which was enhanced by polymer chain ordering of the host P3HT via thermal annealing. The phase-separated film worked as dual-gate transistor channels with clearly different optical responsivities: the top and bottom channels were optically inactive and active, respectively. Therefore, this device configuration can be expected to give multilevel switching with a memory effect. We emphasize that our approach allows the formation of multilayer dual-gate OFETs by a simple one-step spin-coating process and phase separation.

■ ASSOCIATED CONTENT

Supporting Information

Additional results, including transistor properties and TOF-SIMS concerning SP−PTAA blends. This material is available free of charge via the Internet at http://pubs.acs.org.

■ AUTHOR INFORMATION

Corresponding Author

*E-mail: wakayama.yutaka@nims.go.jp.

Notes

The authors declare no competing financial interest.

■ REFERENCES

(1) Walzer, K.; Maennig, B.; Pfeiffer, M.; Leo, K. Highly Efficient Organic Devices Based on Electrically Doped Transport Layers. *Chem. Rev.* **2007**, *107*, 1233−1271.

(2) Meyer, J.; Hamwi, S.; Schmale, S.; Winkler, T.; Johannes, H.-H.; Riedl, T.; Kowalsky, W. A Strategy Towards p-Type Doping of Organic Materials with HOMO Levels beyond 6 eV using Tungsten Oxide. *J. Mater. Chem.* **2009**, *19*, 702−705.

(3) Blochwitz, J.; Pfeiffer, M.; Fritz, T.; Leo, K. Low Voltage Organic Light Emitting Diodes Featuring Doped Phthalocyanine as Hole Transport Material. *Appl. Phys. Lett.* **1998**, *73*, 729−731.

(4) Shinmura, Y.; Kubo, M.; Ishiyama, N.; Kaji, T.; Hiramoto, M. *pn*-control and *pn*-homojunction Formation of Metal-Free Phthalocyanine by Doping. *AIP Adv.* **2012**, *2*, 032145-1-6.

(5) Lee, C.-T.; Chen, H.-C. Performance Improvement Mechanisms of Organic Thin-Film Transistors using MoO_x-Doped Pentacene as Channel Layer. *Org. Electron.* **2011**, *12*, 1852−1857.

(6) Guo, Y.; Liu, Y.; Di, C.; Yu, G.; Wu, W.; Ye, S.; Wang, Y.; Xu, X.; Sun, Y. Tuning the Threshold Voltage by Inserting a Thin Molybdenum Oxide Layer into Organic Field-Effect Transistors. *Appl. Phys. Lett.* **2007**, *91*, 263502-1-3.

(7) Chen, Y.; Shih, I.; Xiao, S. Effects of $FeCl_3$ Doping on Polymer-Based Thin Film Transistors. *J. Appl. Phys.* **2004**, *96*, 454−458.

(8) Schroeder, R.; Majewski, L. A.; Grell, M. Improving Organic Transistor Performance with Schottky Contacts. *Appl. Phys. Lett.* **2004**, *84*, 1004−1006.

(9) Fujimori, F.; Shigeto, K.; Hamano, T.; Minari, T.; Miyadera, T.; Tsukagoshi, K.; Aoyagi, Y. Current Transport in Short Channel Top-Contact Pentacene Field-Effect Transistors Investigated with the Selective Molecular Doping Technique. *Appl. Phys. Lett.* **2007**, *90*, 193507-1-3.

(10) Minari, T.; Miyadera, T.; Tsukagoshi, K.; Aoyagi, Y.; Ito, H. Charge Injection Process in Organic Field-Effect Transistors. *Appl. Phys. Lett.* **2007**, *91*, 053508-1-3.

(11) Li, Y.; Zhang, H.; Qi, C.; Guo, X. Light-Driven Photochromism-Induced Reversible Switching in P3HT−Spiropyran Hybrid Transistors. *J. Mater. Chem.* **2012**, *22*, 4261−4265.

(12) Orgiu, E.; Crivillers, N.; Herder, M.; Grubert, L.; Pätzel, M.; Frisch, J.; Pavlica, E.; Duong, D. T.; Bratina, G.; Salleo, A.; Koch, N.; Hecht, S.; Samorì, P. Optically Switchable Transistor via Energy-Level Phototuning in a Bicomponent Organic Semiconductor. *Nat. Chem.* **2012**, *4*, 675−679.

(13) Andersson, P.; Robinson, N. D.; Berggren, M. Switchable Charge Traps in Polymer Diodes. *Adv. Mater.* **2005**, *17*, 1798−1803.

(14) Lutsyk, P.; Janus, K.; Sworakowski, J.; Generali, G.; Capelli, R.; Muccini, M. Photoswitching of an n-Type Organic Field Effect Transistor by a Reversible Photochromic Reaction in the Dielectric Film. *J. Phys. Chem. C* **2011**, *115*, 3106−3114.

(15) Lutsyk, P.; Janus, K.; Sworakowski, J.; Kochalska, K.; Nešpůrek, S. Kinetic Study of Light-Driven Processes in Photochromic Dye-Doped Polymers used as Gate Insulators in Photoswitchable Organic Field Effect Transistors. *Chem. Phys.* **2012**, *404*, 22−27.

(16) Toman, P.; Bartkowiak, W.; Nešpůrek, S.; Sworakowski, J.; Zaleśny, R. Quantum-Chemical Insight into the Design of Molecular Optoelectrical Switch. *Chem. Phys.* **2005**, *316*, 267−278.

(17) Shen, Q.; Wang, L.; Liu, S.; Cao, Y.; Gan, L.; Guo, X.; Steigerwald, M. L.; Shuai, Z.; Liu, Z.; Nuckolls, C. Photoactive Gate Dielectrics. *Adv. Mater.* **2010**, *22*, 3282−3287.

(18) Guo, X.; Zhang, D.; Yu, G.; Wan, M.; Li, J.; Liu, Y.; Zhu, D. Reversible Photoregulation of the Electrical Conductivity of Spiropyran-Doped Polyaniline for Information Recording and Non-destructive Processing. *Adv. Mater.* **2004**, *16*, 636−640.

(19) Ishiguro, Y.; Hayakawa, R.; Chikyow, T.; Wakayama, Y. Optical Switching of Carrier Transport in Polymeric Transistor with Photochromic Spiropyran Molecules. *J. Mater. Chem. C* **2013**, *1*, 3012−3016.

(20) Ishiguro, Y.; Hayakawa, R.; Yasuda, T.; Chikyow, T.; Wakayama, Y. Unique Device Operations with a Combination of Optical-Memory Effect and Electrical-Gate Modulation in a Photochromism-Based Dual-Gate Transistor. *ACS Appl. Mater. Interfaces* **2013**, *5*, 9726−9731.

(21) Yang, F.-Y.; Chang, K.-J.; Hsua, M.-Y.; Liu, C.-C. High-Performance Poly(3-Hexylthiophene) Transistors with Thermally Cured and Photo-Cured PVP Gate Dielectrics. *J. Mater. Chem.* **2008**, *18*, 5927−5932.

(22) Baillet, G.; Giusti, G.; Guglielmetti, R. Comparative Photodegradation Study between Spiro[Indoline−Oxazine] and Spiro-[Indoline−Pyran] Derivatives in Solution. *J. Photochem. Photobiol., A* **1993**, *70*, 157−161.

(23) Arai, K.; Shitara, Y.; Ohyama, T. Preparation of Photochromic Spiropyrans Linked to Methyl Cellulose and Photoregulation of Their Properties. *J. Mater. Chem.* **1996**, *6*, 11−14.

(24) Pimienta, V.; Lavabre, D.; Levy, G.; Samat, A.; Guglielmetti, R.; Micheau, J. C. Kinetic Analysis of Photochromic Systems under Continuous Irradiation. Application to Spiropyrans. *J. Phys. Chem.* **1996**, *100*, 4485−4490.

(25) Moritani, K.; Mukai, G.; Hashinokuchi, M.; Mochiji, K. Energy-Dependent Fragmentation of Polystyrene Molecule using Size-Selected Ar Gas Cluster Ion Beam Projectile. *Surf. Interface Anal.* **2011**, *43*, 241−244.

(26) Lee, W. H.; Lim, J. A.; Cho, J. H.; Lee, H. S.; Choi, H. H.; Cho, K. Semiconductor-Dielectric Blends: A Facile All Solution Route to Flexible All-Organic Transistors. *Adv. Mater.* **2009**, *21*, 4243−4248.

(27) Hwang, D. K.; Fuentes-Hernandez, C.; Berrigan, J. D.; Fang, Y.; Kim, J.; Potscavage, W. J., Jr.; Cheun, H.; Sandhage, K. H.; Kippelen, B. Solvent and Polymer Matrix Effects on TIPS-Pentacene/Polymer Blend Organic Field-Effect Transistors. *J. Mater. Chem.* **2012**, *22*, 5531−5537.

(28) Madec, M.-B.; Crouch, D.; Llorente, G. R.; Whittle, T. J.; Geoghegan, M.; Yeates, S. G. Organic Field Effect Transistors from Ambient Solution Processed Low Molar Mass Semiconductor−Insulator Blends. *J. Mater. Chem.* **2008**, *18*, 3230−3236.
(29) Qiu, L.; Lim, J. A.; Wang, X.; Lee, W. H.; Hwang, M.; Cho, K. Versatile Use of Vertical-Phase-Separation-Induced Bilayer Structures in Organic Thin-Film Transistors. *Adv. Mater.* **2008**, *20*, 1141−1145.
(30) Kang, J.; Shin, N.; Jang, D. Y.; Prabhu, V. M.; Yoon, D. Y. Structure and Properties of Small Molecule−Polymer Blend Semiconductors for Organic Thin Film Transistors. *J. Am. Chem. Soc.* **2008**, *130*, 12273−12275.
(31) Smith, J.; Hamilton, R.; McCulloch, I.; Stingelin-Stutzmann, N.; Heeney, M.; Bradleya, D. D. C.; Anthopoulos, T. D. Solution-Processed Organic Transistors Based on Semiconducting Blends. *J. Mater. Chem.* **2010**, *20*, 2562−2574.